ARTICLES

Magnetic susceptibility and heat-capacity studies of $NiS_{2-x}Se_x$ single crystals: A study of transitions at nonzero temperature

X. Yao
Department of Chemistry, Purdue University, West Lafayette, Indiana 47907-1393

Y.-K. Kuo,* D. K. Powell, and J. W. Brill
Department of Physics and Astronomy, University of Kentucky, Lexington, Kentucky 40506-0055

J. M. Honig
Department of Chemistry, Purdue University, West Lafayette, Indiana 47907-1393
(Received 18 February 1997)

Heat-capacity and magnetic-susceptibility studies have been carried out on $NiS_{2-x}Se_x$ single crystals for $0.38 \leqslant x \leqslant 0.58$ and $0 \leqslant x \leqslant 0.71$, respectively. These and earlier physical measurements document the gradual evolution, with rising x, of the alloys from good insulators to poor metals at low temperatures. The transitions between various magnetically ordered or disordered phases are marked by anomalies in these physical measurements. The trend of magnetic susceptibility with temperature indicates that alloys near the crossover to the highly correlated metallic state exhibit increasing charge-carrier localization with rising temperature; this is ascribed to the dominance of entropic contributions to the free energy. It is stressed that these variations in properties are achieved by isoelectronic substitutions in the anion sublattice that leave the cation sublattice undisturbed. [S0163-1829(97)08535-4]

INTRODUCTION

The $NiS_{2-x}Se_x$ system is currently under intensive investigation because one can generate substantial changes in the electronic properties while keeping the cationic configuration and pyrite structure intact. By contrast, in most other alloy systems [e.g., V_2O_3 (Ref. 1)] such alterations are achieved only by replacement of the host cations by altervalent substituents. In the present work, the correlation effects associated with the $3d$ cationic states are therefore essentially unperturbed by the substitutional disorder in the anionic sublattice.

Selenium can be substituted for sulfur at all concentrations in the compound under investigation.[2] Since S and Se are isovalent, the density of the valence electrons remains constant as x is varied; nevertheless, NiS_2 is a Mott insulator while $NiSe_2$ is a reasonably good paramagnetic metal. Thus, one would anticipate an intermediate composition range in which the alloys display a range of distinct characteristics as the temperature is altered. Pioneering, as well as follow-up studies on the $NiS_{2-x}Se_x$ system do show a rich variety of properties in the region $0 \leqslant x < 1$,[2–27] manifested in the phase diagram shown in Fig. 1, which was recently reviewed by Sudo.[16] Typically, the alloys exhibit a temperature-induced metal-insulator transition for $x < 0.7$. The alloys are paramagnetic at room temperature but undergo antiferromagnetic ordering at temperatures $T < 100$ K. Additionally, compounds with relatively lower Se content, when further cooled, undergo a transformation from antiferromagnetism to a canted spin structure, giving rise to parasitic ferromagnetism. In pure NiS_2 the canting angle is of the order of 0.1°.[18] There is disagreement on the precise positioning of the phase boundaries and on the largest x value to which the weak ferromagnetic state extends,[4,5,10,13,14,16,19,21,22] as is discussed further below.

Most prior investigations have been carried out on polycrystalline specimens; the corresponding transport measurements are sensitive to surface or intergrain structures, as has recently been demonstrated on NiS_2.[18] Single-crystal investigations before 1994 were executed on alloys grown by chemical vapor transport techniques in which it is difficult to avoid incorporation of the transporting agents. In addition, deviations from the ideal 2/1 anion/cation ratio may play an important role.

In light of the above, we initiated systematic studies on single crystals grown in a tellurium flux, as described elsewhere.[17] No Te incorporation was detected by microprobe analysis, sensitive to 0.1% by weight. Since Te is isovalent to S and Se, small traces of the flux in the host should give rise only to secondary effects.

The present paper is an extension of electrical transport measurements reported in Refs. 23 and 24. Here we present and discuss heat-capacity and magnetization measurements on $NiS_{2-x}Se_x$ single crystals in the range $0 \leqslant x \leqslant 0.71$, in which the various metal-insulator transitions of interest occur. This study provides further insight into the electronic state and phase transitions in this set of materials.

EXPERIMENTAL DETAILS

As-grown crystals[17] of $NiS_{2-x}Se_x$ varied from roughly cubic ($\approx 1\ mm^3$) to platelike ($\approx 1 \times 0.1 \times 0.01\ mm^3$) in

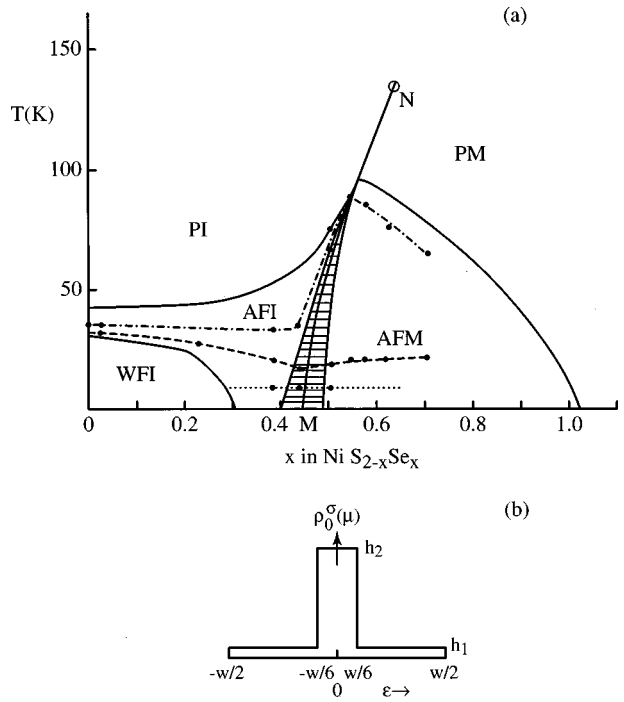

FIG. 1. (a) The solid curves show the phase diagram of $NiS_{2-x}Se_x$ as assembled from data in the literature; see text. The hatched region indicates uncertainties in the placement of the metal-insulator boundaries. The points are taken from the heat-capacity and magnetic-susceptibility data of the present work. The dot-dashed lines show our proposed AFI-PI boundary and the dashed lines show our proposed boundary of the weak ferromagnetic regime, extending beyond $x=0.30$. The dotted lines shows the possible low-temperature transition suggested by the heat-capacity measurements. (b) Schematic density of states used in calculations of Appendix A.

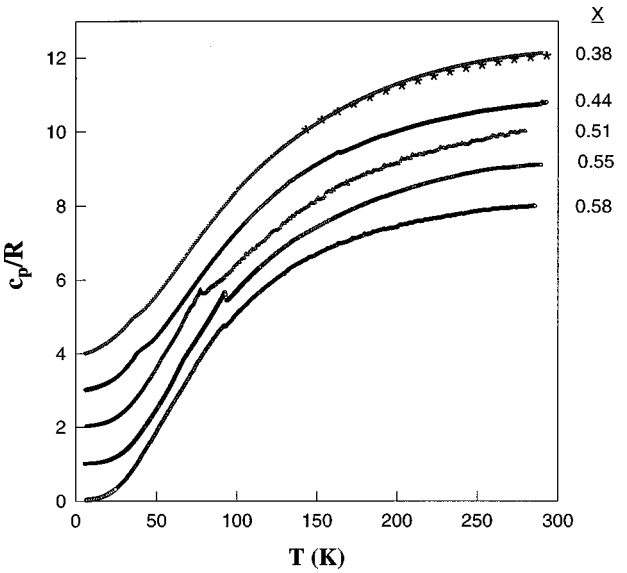

FIG. 2. Molar heat capacity (c_P), normalized to the gas constant (R), vs temperature for crystals of $NiS_{2-x}Se_x$ single crystals for indicated x values. Successive graphs are offset by 1 unit. The stars show the differential scanning calorimetry results for an $x=0.38$ powder.

shape. We assumed that the x values of the samples were the same as those of the starting materials, as was checked by comparison of the lattice parameters of various alloys to values cited in Ref. 2. Using calibrated microprobe techniques, the (S+Se)/Ni ratio was found to fall between 1.98 and 2.02.

Standard magnetic-susceptibility measurements were carried out with a SQUID magnetometer using platelet-shaped material, with the applied magnetic field of 1-T oriented perpendicular to the flat faces of the crystals. No corrections were made for the underlying diamagnetism, which is at least an order of magnitude smaller than the paramagnetic susceptibilities, or for demagnetizing effects, since the magnetization is small even in the ferromagnetic state. Some magnetization measurements were carried out on two samples from the same batch, with no significant differences in the results.

Heat capacities were measured using an ac calorimetric technique described by Chung *et al.*[25] Photoabsorbing PbS films were evaporated on the samples, which were cubic crystals sanded to a thickness ≈ 0.1 mm to reduce their thermal time constants. In the experiment, the samples were heated by chopped light, and the average and oscillating temperatures were measured with thermometers attached to the back surface with varnish; type E thermocouples,[26] chromel/Au(Fe) thermocouples, and thin-film bolometers[27] were used in different temperature ranges. For appropriately chosen chopping frequencies, typically 3–12 Hz, the magnitude of the temperature oscillation is inversely proportional to the total heat capacity of the sample and addenda.[25,28] The molar heat capacity, c_p, of the sample, corrected for the addenda, was normalized to the value established by differential scanning calorimetry[29] (DSC) on powder at 200 K. In the over-

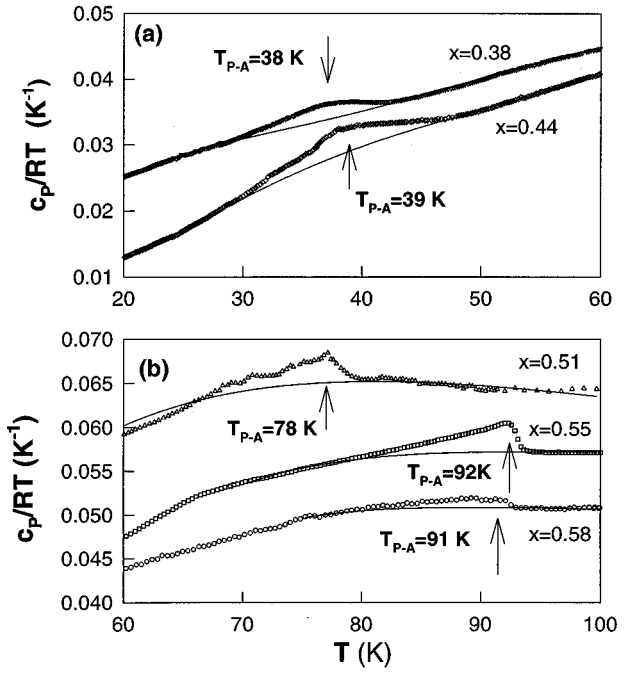

FIG. 3. c_P/RT vs temperature near the paramagnetic to antiferromagnetic transitions, shown by arrows. (a) Semiconducting samples; data for $x=0.38$ are offset by $0.01\,K^{-1}$. (b) Metallic samples; data for $x=0.55$ and 0.51 are offset by 0.01 and $0.02\,K^{-1}$, respectively.

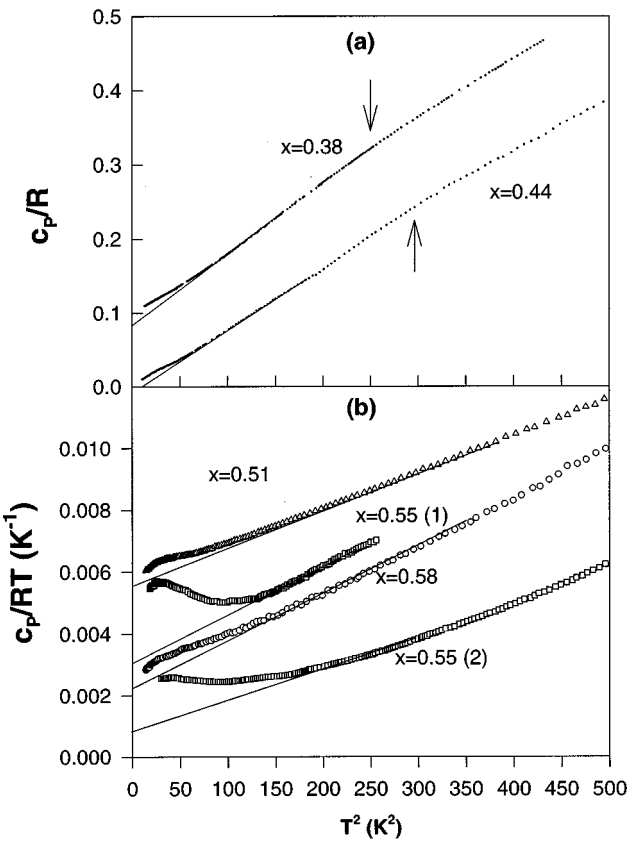

FIG. 4. Molar heat capacities at low temperature. (a) c_P/R vs T^2 for semiconducting samples. Data for $x=0.38$ are offset by 0.1. Light lines show extrapolations of $c_P=\alpha T^2$ behavior. Arrows indicate slope changes associated with the weak ferromagnetic to antiferromagnetic transitions. (b) c_P/RT for metallic samples. Data for $x=0.51$ (only) is offset by 0.003 K^{-1}. Light lines show extrapolations of $c_P=\beta T^3+\gamma T$ behavior.

lapping temperature range $T>130$ K, the DSC and ac calorimetry results agreed to within 2%, as indicated for the $x=0.38$ composition in Fig. 2. Measurements were carried out for two samples each of stoichiometry $x=0.38$, 0.44, 0.51, 0.55, and 0.58. For the latter three compositions, the results were somewhat sample dependent, reflecting the sensitivity of properties to changes in sample stoichiometry, surface states, and the steep rise (cf. Fig. 1) of the phase boundary separating the metallic and insulating states.

HEAT-CAPACITY STUDIES

As far as we know, the only prior heat-capacity measurements were executed by Sudo and co-workers[19] on polycrystalline samples with $x=0.51$ and 0.52. In Fig. 2, we present molar heat capacities on single crystals; the various curves are offset as stated in the caption. The general temperature dependence is very similar to that reported by Sudo *et al.*[19] We observe small anomalies which are shown in more detail in Fig. 3; note the offsets described in the captions. Second specimens with $x=0.51$ and 0.58 did not show these anomalous peaks, but the second $x=0.58$ sample did exhibit a much smaller peak near 75 K. Again, this indicates the sensitivity of specimens to stoichiometry and surface conditions. We also note that the c_p peak measured by Sudo *et al.* for

TABLE I. Listing of transition temperatures for $NiS_{2-x}Se_x$ single crystals for the weak ferromagnetic (WF) to antiferromagnetic (AF) transition and antiferromagnetic to paramagnetic (P) transition observed in the heat-capacity and magnetic-susceptibility measurements.

	Transition based on heat-capacity measurements T_c (K)		Transition based on magnetization measurements T_c (K)	
x	WF-AF	AF-P	WF-AF	AF-P
0			35	38
0.03			31	35
0.24			28	34
0.38	16	38	20	33
0.44	17	39	19	35
0.51		78	19	65
0.55		92	21	92
0.58		91	21	90
0.63			21	77
0.71			21	68

their $x=0.51$ and 0.52 samples were located at $T\approx 38$ K, where we observe comparable anomalies for samples with x in the range 0.38–0.44, which have semiconducting ground states with resistivities at $T=4$ K in the 10^3 Ω cm range.[23] Sudo *et al.* further reported a hysteresis of ≈ 1 K and a corresponding latent heat of 38 J/mol$\approx RT_c/8$.[19] ac calorimetry techniques are not sensitive to latent heat effects;[25] however, no hysteresis ($\Delta T<0.1$ K) was detected by us in electrical, magnetic, and thermal measurements and the c_P anomalies in our measurements are of the type normally associated with broadened, mean-field transitions of second or higher order. Neutron scattering studies carried out on NiS_2 also yielded critical exponents consistent with mean-field theory.[18]

As discussed below, the temperatures of these c_P anomalies, listed in Table I; correlate with changes in the magnetic properties associated with the antiferromagnetic to paramagnetic transition. The magnitudes of our c_P peaks, estimated using the backgrounds shown, range from $\Delta c_P\approx R/12$ to $R/3$ (i.e., 0.75 to 2.5 J/mol K). The molar magnetic entropy change is expected to be $\Delta s=[R\ \ln(2S+1)]$, where S is the spin, but estimating Δs from the specific heat depends critically on the placement of the background curve of the latter. However, for a mean-field transition, $\Delta s=\Delta c_P/1.43$; i.e., Δs would range from $R/17$ to $R/4$ for our samples. Similarly, even when choosing a background well below their measured specific heat, Sudo *et al.*[19] obtained a magnetic entropy of only 1.7 J/mol K ($\approx R/5$). These small values of Δs may reflect heterogeneous broadening of the transitions and/or reduced Ni magnetic moments (as assumed by Sudo *et al.*[19]).

The low-temperature variations of the molar heat capacities are shown in Fig. 4 (note the offsets listed in the caption) as plots of c_P vs T^2 for samples with $x<0.5$ (upper panel) and c_P/T vs T^2 for samples with $x>0.5$ (lower panel). Results are shown for both $x=0.55$ samples, which had very similar behavior at high temperature (including anomalies at

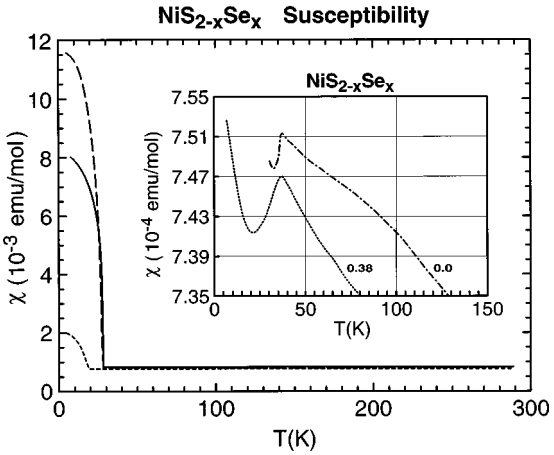

FIG. 5. Magnetic susceptibility vs temperature for $NiS_{2-x}Se_x$ single crystals with composition $0 \leqslant x \leqslant 0.24$. Solid curve: $x=0.0$; Long dashed curve: $x=0.03$; Short dashed curve: $x=0.24$. Inset shows the variations on an expanded scale.

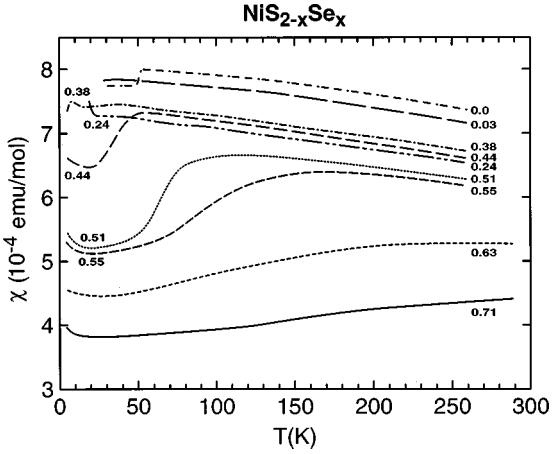

FIG. 6. Variation of magnetic susceptibility with temperature for $NiS_{2-x}Se_x$ single crystals in the range $0 \leqslant x \leqslant 0.71$.

92 K), but exhibit rather different low-temperature behavior. For all samples, small anomalies, discussed further below, are observed near 6 K.

For the metallic ($x>0.5$) samples, the anticipated Sommerfeld behavior, $c_P=\gamma T+\beta T^3$, holds above the low-temperature anomalies. β/R varies from 1.1×10^{-5} K^{-4} to 1.5×10^{-5} K^{-4}, corresponding to a Debye temperature of $\Theta_D \approx 380$ K, as found by Sudo *et al.*[19] The values of γ are 22, 25, 6, and 20 mJ K^{-2} mol^{-1} for $x=0.51$, 0.55(1), 0.55(2), and 0.58, respectively. Note the very small value of γ for the $x=0.55(2)$ specimen, comparable to that of standard metals, for which we have no explanation. The other values of γ, which lie in the range of moderately to highly correlated metals [e.g., (highly correlated) V_2O_3 has $\gamma=60$ mJ K^{-2} mol^{-1}],[1] are slightly smaller than that reported by Sudo and co-workers.[19]

Between 7 K (i.e., above the anomalies) and 16 K, $c_P \propto T^2$ for the semiconducting ($x=0.38$ and $x=0.44$) samples. According to standard theory, c_P should vary as $T^{3/2}$ or T^3, depending on whether (ferromagnetic) magnon or phonon excitation predominates; however, fits of $c_P/T^{3/2}$ vs $T^{3/2}$ were much worse than the fits shown in Fig. 4(a). The observed $c_P \propto T^2$ behavior may be rationalized by noting that frustration dominates the magnetic interactions and that the ferromagnetism is parasitic. In such circumstances, a power-law exponent between 3/2 and 3 is reasonable. There are distinct changes in slope (indicated by the arrows) at 16 and 17 K, for the $x=0.38$ and 0.44 specimens, respectively, which are more obvious in plots of c_P/T vs T. These are close to the temperatures of the minima in susceptibility (20 and 19 K; see Table I and Figs. 5 and 6, below) that we associate with the weak ferromagnetic to antiferromagnetic transition, as discussed below. However, no corresponding c_P anomalies are observed for the metallic samples, which also have magnetic anomalies at similar temperatures.

We now discuss the small anomalies in c_P observed for all samples near 6 K; similar behavior was observed by Sudo *et al.*[19] If one estimates the entropy involved by extrapolating the higher-temperature behavior [αT^2 or ($\beta T^3+\gamma T$)], as shown in Fig. 4, one finds that, in all cases, the entropy change $\int \Delta c_P dT/T < 0.02R$. We mention three possible explanations for these anomalies, although all are problematic: (i) The low-temperature specific heat is augmented by paramagnon excitation, which for a correlated metal has the form[19,30] $c_{para}=\delta T^3 \ln(T/T_0)$; such an effect has been reported for $LaNiO_3$.[31] In our case, the peaks in c_P/T near 6 K imply a spin-flip temperature of $T_0 \approx 10$ K. The difficulty with this interpretation, as discussed by Sudo,[16] is that paramagnon excitation should only occur in the paramagnetic state, and not in the magnetically ordered state observed for $NiS_{2-x}Se_x$ at these temperatures. (ii) The anomalies are Schottky anomalies associated with defect states. In this case, the largest anomaly [for the $x=0.55$ (1) sample] $\int \Delta c_P dT/T \approx 0.02R$ would imply an extremely large defect concentration of $0.02/\ln(2) \approx 3\%$. (iii) The anomalies reflect new low-temperature transitions. The small size of the anomalies indicate that the change in order would be very subtle. We note that no anomalies near 6 K have been observed in other properties.[23]

MAGNETIC-SUSCEPTIBILITY RESULTS

The magnetic characteristics of $NiS_{2-x}Se_x$ have been previously investigated by NMR,[6,11] Mössbauer spectroscopy,[20] and magnetization measurements;[13,16,21] only the magnetization studies of Sudo and Miyadai[13] extended over an appreciable composition range. Since those measurements were performed on sintered powders, it seemed desirable to check their interesting results on single crystals and to extend the composition range. The results are discussed under three headings.

(a) $0 \leqslant x \leqslant 0.24$. Figure 5 shows a plot of the molar susceptibilities, χ vs temperature for samples with low-x values. One should note the steep rise in χ with diminishing T below 30 K, characteristic of a weak ferromagnetic insulator (WFI), with a leveling off of χ in the cryogenic temperature range, as described by Carlin.[32] Unlike Sudo and Miyadai,[13] we do not observe any large saturated magnetization in the WFI state. This may reflect the fact that the canting of the antiferromagnetically aligned spins may be much larger in surface regions than in the crystal bulk, leading to enhanced values of magnetization in polycrystalline materials.

Nevertheless, the susceptibilities computed by Sudo and Miyadai,[13] after subtraction of the remanent magnetizations,

agree well with those we observe. In the paramagnetic state, discussed below, our susceptibilities are typically 5–10 % below those of Ref. 13; as shown by Thio, Bennett, and Thurston[18] for NiS_2, the difference may be associated with enhanced surface magnetism in the polycrystalline samples.

The sharp break which separates the steeply rising and flat portions of the data delineates the transition to the antiferromagnetic insulating (AFI) state at higher temperature. Beyond 30 K, χ varies weakly with temperature, as is shown in the inset to Fig. 5 on very much enlarged temperature and susceptibility scales. One should note the minimum separating the AFI and WFI regions, which is a signature of a pseudocompensation point, normally associated with the disappearance of the parasitic ferromagnetic phase. After all the moments have been aligned antiparallel, the susceptibility grows with increasing temperature until the Néel point is reached, beyond which χ drops with rising temperature. The maximum in slope is therefore taken as the Néel point.

It should be reemphasized that the temperature variation of the susceptibility beyond 30 K is very small. This result is somewhat unexpected because the resistivities of crystals in this composition range are typical of highly insulating phases.[23] Since the Curie-Weiss law is not obeyed, we conclude that no localized moments exist on Ni sites. In fact, the nickel-chalcogenide bonding is far more covalent than in the nickel oxide series; the strong admixtures of cationic and anionic states result in relatively wide bands that render carriers itinerant. This is in consonance with the small Seebeck coefficients reported for these alloys even at low temperatures.[23] The nearly constant value of χ for $T>30$ K may be ascribed to van Vleck paramagnetism. On setting $\chi = 2N_A\langle\mu\rangle^2/\Delta = 7.5\times10^{-4}$ emu/mol, where N_A is Avogadro's number, and taking the matrix element $\langle\mu\rangle \approx \mu_B$, the Bohr magneton, the gap is calculated to be of the order of 300 meV, in reasonable agreement with twice the measured conductivity activation energy of 110 meV, cited by Yao *et al.*[23] for $T>70$ K. The temperature variation of χ is also shown by the top three curves in Fig. 6.

(b) $0.38\leqslant x\leqslant 0.55$. Here the susceptibilities, shown in Fig. 6, fall below those of set (a). One again encounters a definite minimum in the χ vs T plots near 20–30 K, depending on x, which we interpret as pseudocompensation points, separating weak ferromagnetic from antiferromagnetic spin alignment. This is followed by a marked rise in χ with temperature up to a maximum, beyond which χ drops slightly with rising T. The Néel points are read off from the maximum values of $d\chi/dT$ and are entered in Table I: these coincide fairly well with the locations of the respective heat-capacity anomalies.

One should note the unusually wide temperature ranges of increasing χ, associated with the transition from antiferromagnetism to paramagnetism, especially as the upper bound of this composition range is reached. We believe that these reflect a change in the qualitative nature of the electronic systems, as described in Refs. 23 and 24 on the basis of resistivity and Seebeck coefficient measurements. Metallic compounds in this range of composition are highly correlated; as previously described,[33] relative to the completely localized state, carriers in such narrow-band systems have a negative kinetic energy which is nearly counterbalanced by their mutual positive interaction energy. In such circumstances, the entropy of the carriers assumes an important role. For localized electrons filling exactly half the available states in a paramagnet, the spin degeneracy gives rise to an entropy per electron of $k_B \ln 2$, whereas the entropy of the itinerant (Fermi or statistical) spin liquid is much smaller at low temperatures. In these circumstances, the system tends to move toward a more localized state (with free energy $-k_BT \ln 2$) at high temperature. This localization manifests itself in the narrowing of energy bands and in the opening of a band gap and is reflected in a large increase of the resistivity with temperature before a maximum is reached in the range 50–100 K.[23,24] It also give rise to an increase in the magnetic moment of the nickel ion and, hence, to the observed rise in susceptibility with temperature. The flattening out of χ with T beyond 50–100 K, depending on alloy composition, is also roughly coincident with the maximum reached in the resistivity vs temperature variation.

(c) $0.58\leqslant x\leqslant 0.71$. Here one still encounters a shallow minimum near 30 K whose interpretation is less clear, but likely still indicative of a pseudocompensation point. The maximum in $d\chi/dT$ diminishes rapidly with increasing x. Beyond this maximum, χ continues to rise slightly with T, by roughly 10% over a 200-K temperature interval. The resistivities remain in the 10^{-3} Ω cm range,[23,24] which classifies the materials as poor metals. Theories pertaining to highly correlated metals[33] show that their magnetic susceptibilities should be almost independent of temperature; see also Appendix A. However, their χ values should also be larger than those of standard Pauli paramagnetic metals, as is the case here. In Appendix A, we provide a sample calculation that rationalizes these observations and the overall consistency of the theoretical analysis.

CONCLUSIONS

The data presented here suggest an amendment of the commonly accepted phase diagram. The phase boundaries as determined by the heat-capacity and magnetic-susceptibility anomalies are entered as points on the phase diagram shown in Fig. 1. The chief difference between the present and earlier versions is that, based on the minima in χ near 30 K, we extend the ferromagnetic phase to a composition range well beyond the customarily accepted limit of $x=0.30$. Failure to detect this phase in earlier neutron-diffraction experiments,[13,16,36] would indicate that the aligned magnetic moments on the cations are very small, and hence the weak intensity of the magnetic reflections might have remained undetected in samples with $x>0.30$. The other features of the phase diagram which we propose are in fair concordance with previously established phase boundaries; as stated earlier, their placement has been uncertain because of disagreements among various investigators.

In summary, we have shown in this and in prior work[23,24] that a progressive increase in Se content of $NiS_{2-x}Se_x$ in the range $0\leqslant x\leqslant 0.71$ changes the alloy in the low-temperature regime from an insulator to a correlated metal. Transitions or crossovers between the various phases indicated in Fig. 1 are reflected in anomalies in various transport, magnetic, and thermal characteristics. Present and earlier work by others has shown that these characteristics are very dependent on sample preparation techniques. It is remarkable that such di-

versity of properties can be achieved by isoelectronic replacement of S by Se, which in the first approximation only involves an increasing degree of cation-anion orbital overlap in the lattice constituents.

ACKNOWLEDGMENTS

The research at Purdue University was supported by NSF Grant No. DMR-92-22986. The research at the University of Kentucky was supported by NSF Grant Nos. EHR-91-08764 and DMR-93-00507. Very useful discussions with Professor J. Appel, University of Hamburg, and Professor J. Spałek, Jagiellonian University, Krakow, are gratefully acknowledged.

APPENDIX A: THEORETICAL ANALYSIS

The sample calculations shown here are based on a treatment by Spałek and co-workers[33] of electron correlation phenomena in conductors at nonzero temperatures. The theory applies to a nondegenerate band which is exactly half filled. In the limit of low temperatures, the electronic contribution to the molar heat capacity is given by

$$c_P=\gamma_0 T/(1-I^2)\equiv\gamma T=[2.94\times10^{16}\rho_0^\sigma/(1-I^2)]T. \tag{A1}$$

Here $\gamma_0=2\pi^2k_B^2N_A\rho_0^\sigma/3$ is the Sommerfeld constant and ρ_0^σ the density of states (per spin) at the bare electron Fermi level. $I\equiv U/U_c$, where U is the intraatomic electronic repulsion energy and $U_c=8|\overline{\epsilon}|$ is its critical value, related to the average kinetic energy, ϵ, of the noninteracting electron assembly. The numerical factor holds when energies are expressed in eV. At low temperatures, the electronic contribution to the heat capacity is linear, as for uncorrelated electrons, but the Sommerfeld constant is enhanced by the factor $(1-I^2)^{-1}$ through correlation effects.

The magnetic susceptibility in the paramagnetic regime is given by

$$\chi=2\mu_B^2N_A\rho_0^\sigma/[(1-I^2)S], \tag{A2}$$

where S is the Stoner enhancement factor given by

$$S=1-\rho_0^\sigma U(1+I/2)/(1+I)^2. \tag{A3}$$

In the approximation used here, the susceptibility is independent of temperature, as for the free-electron gas. However, the normal Pauli susceptibility is enhanced by the factor $[(1-I^2)S]^{-1}$. The ratio

$$\gamma/\chi=1/3(\pi k_B/\mu_B)^2S=7.27\times10^8S \tag{A4}$$

yields S directly; the numerical factor applies when χ is expressed in emu/mol and c_P in erg/mol K^2.

Numerical evaluations have as their goal the specification of ρ_0^σ, U, and W, the bare electron bandwidth. In the absence of sufficient independent experimental data, we will adopt the density of states, illustrated in Fig. 1(b), which simulates the peaked density of states which is thought to dominate the electronic properties of conductors at the verge of a transition to the Mott state.[34] As shown in Ref. 35, this density of states yields an estimate of $\rho_0^\sigma=3/W$ and $\overline{\epsilon}=-W/12$, in the limit where the central peak is large compared to the wings. Then Eqs. (A1) and (A4), with representative values of $\gamma=2.5\times10^5$ ergs/mol K^2 and $\chi=6.2\times10^{-4}$ emu/mol, yield the estimates $\rho_0^\sigma=4.7$/eV spin, $U=0.15$ eV, and $W=0.64$ eV. The exchange energy and Néel temperature can then be estimated[33] as $J=W^2U/(ZU_c)^2=2.3$ meV and $T_N=ZJ/4k_B=82$ K, where $Z=12$ is the number of nickel nearest neighbors. These sample calculations should not be taken too literally, but the reasonable values obtained do indicate the self-consistency of the approach. More meaningful numerical estimates must await the separate determination of ρ_0^σ through measurements such as x-ray or ultraviolet photoemission spectroscopy.

*Current address: Department of Physics, Clemson University, Clemson, SC 29631.

[1] S. A. Carter *et al.*, Phys. Rev. B **43**, 607 (1991).
[2] D. D. Klemm and N. Jahr, Miner. Monat. **1962**, 32 (1962).
[3] R. J. Bouchard, J. L. Gillson, and H. S. Jarrett, Mater. Res. Bull. **8**, 489 (1973).
[4] H. S. Jarrett *et al.*, Mater. Res. Bull. **8**, 877 (1973).
[5] G. Czjzek *et al.*, J. Magn. Magn. Mater. **3**, 58 (1976).
[6] G. Krill *et al.*, J. Phys. (Paris) Colloq. **37**, C4-23 (1976).
[7] G. Krill and A. Amamou, J. Phys. Chem. Solids **41**, 531 (1980).
[8] P. Kwizera, M. S. Dresselhaus, and D. Adler, Phys. Rev. B **21**, 2328 (1980).
[9] V. Lemos *et al.*, Phys. Status Solidi B **100**, 755 (1980).
[10] H. Takano and A. Okiji, J. Phys. Soc. Jpn. **50**, 3835 (1981).
[11] Y. Kitaoka, H. Yasuoka, and S. Ogawa, J. Phys. Soc. Jpn. **51**, 2707 (1982).
[12] N. Mōri and H. Takahashi, J. Magn. Magn. Mater. **31-34**, 335 (1983).
[13] S. Sudo and T. Miyadai, J. Phys. Soc. Jpn. **54**, 3934 (1985).
[14] F. Gautier *et al.*, Phys. Lett. **53A**, 31 (1975).
[15] T. Miyadai, M. Saitoh, and Y. Tazuke, J. Magn. Magn. Mater. **104-107**, 1953 (1992).
[16] S. Sudo, J. Magn. Magn. Mater. **114**, 57 (1992).
[17] X. Yao and J. M. Honig, Mater. Res. Bull. **29**, 709 (1994).
[18] T. Thio, J. W. Bennett, and J. R. Thurston, Phys. Rev. B **52**, 3555 (1995).
[19] S. Sudo *et al.*, J. Phys. Soc. Jpn. **55**, 1806 (1986); T. Miyadai *et al.*, J. Phys. (Paris) Colloq. **49**, C8-187 (1988). (Note that the ordinates in the c_P vs T graphs in these papers should be multiplied $\times10^3$.)
[20] Y. Nishihara, S. Ogawa, and S. Waki, J. Phys. C **11**, 1935 (1978).
[21] T. Miyadai *et al.*, J. Magn. Magn. Mater. **31-34**, 337 (1983).
[22] S. Ogawa, J. Appl. Phys. **50**, 2308 (1979).
[23] X. Yao *et al.*, Phys. Rev. B **54**, 17 469 (1996); in *The Metal-Nonmetal Transition Revisited*, edited by P. P. Edwards and C. N. R. Rao (Taylor and Francis, London, 1995), p. 127 ff.
[24] X. Yao *et al.*, Mater. Res. Bull. (to be published).
[25] M. Chung *et al.*, Phys. Rev. B **48**, 9256 (1993).
[26] M. Chung and J. W. Brill, Rev. Sci. Instrum. **64**, 2037 (1993).
[27] Y.-K. Kuo, Ph.D. thesis, University of Kentucky, 1995.
[28] R. F. Sullivan and G. Seidel, Phys. Rev. **173**, 679 (1968).
[29] Y. Wang *et al.*, Synth. Met. **46**, 307 (1992).
[30] C. J. Pethick and G. M. Carneiro, Phys. Rev. A **7**, 304 (1973); J. W. Rasul and T. Li, J. Phys. C **21**, 5119 (1988); T. Li and P. Wöfle, Z. Phys. B **78**, 45 (1990).
[31] K. Sreedhar *et al.*, Phys. Rev. B **46**, 6382 (1992).

[32] R. L. Carlin, *Magnetochemistry* (Springer Verlag, Berlin, 1986), p. 142 ff.

[33] J. Spałek and A. M. Oleś, Physica B&C **86-88**, 375 (1977); K. A. Chao *et al.*, J. Phys. (Paris) Colloq. **20**, C-27 (1977); J. Spałek, A. M. Oleś, and K. A. Chao, Phys. Status Solidi B **108**, 329 (1981); J. Spałek, A. M. Oleś, and J. M. Honig, Phys. Rev. B **28**, 6802 (1983); J. Spałek, A. Datta, and J. M. Honig, Phys. Rev. Lett. **59**, 128 (1987); J. Spałek, M. Kokowski, and J. M. Honig, Phys. Rev. B **39**, 9175 (1989); J. Spałek *et al.*, Solid State Commun. **70**, 911 (1989); J. Spałek, J. Solid State Chem. **88**, 70 (1990).

[34] W. Metzner and D. Vollhardt, Phys. Rev. Lett. **62**, 324 (1989); E. Müller-Hartmann, Z. Phys. B **74**, 507 (1989); E. Müller-Hartmann, Int. J. Mod. Phys. B **3**, 2169 (1989); M. Rozenberg, X. Y. Zhang, and G. Kotliar, Phys. Rev. Lett. **69**, 1236 (1992); A. Georges and W. Krauth, *ibid.* **69**, 1240 (1992); M. Jarrell, *ibid.* **69**, 168 (1992); X. Y. Zhang, M. J. Rozenberg, and G. Kotliar, *ibid.* **70**, 1666 (1993); Th. Pruschke, D. L. Cox, and M. Jarrell, Phys. Rev. B **47**, 3553 (1993); M. J. Rozenberg, G. K. Kotliar, and X. Y. Zhang, *ibid.* **49**, 10 181 (1994).

[35] A. Datta, J. M. Honig, and J. Spałek, Phys. Rev. B **44**, 8459 (1991).

[36] T. Miyadai *et al.*, Phys. Lett. **44A**, 529 (1973); J. Phys. Soc. Jpn. **38**, 115 (1975); Physica B&C **86-88**, 901 (1977); Phys. Lett. **67A**, 61 (1978); P. Plumier and G. Krill, J. Phys. (France) Lett. **36**, L249 (1975); K. Kikuchi *et al.*, J. Phys. Soc. Jpn. **45**, 444 (1978); P. Pannisod *et al.*, Solid State Commun. **29**, 67 (1979).